

DISPERSION EFFECTS IN CAPILLARY ZONE ELECTROPHORESIS

GLYN O. ROBERTS*

Roberts Associates, Inc., 380 West Maple Avenue, Suite L-1A, Vienna, VA 22180 (U.S.A.)

and

PERCY H. RHODES and ROBERT S. SNYDER

George C. Marshall Space Flight Center, National Aeronautics and Space Administration, Code ES76, Huntsville, AL 35812 (U.S.A.)

SUMMARY

We quantitatively analyzed possible causes of the observed spreading of sample components which degrades separation compared with theoretical limits, and identified four potentially significant causes, electrokinetic dispersion, wall adsorption, enhanced diffusion due to Poiseuille flows driven by pressure gradients, and enhanced diffusion due to mobility variations associated with transverse temperature differences. Electrokinetic dispersion is caused by changes in the conductivity and pH distributions, proportional to the concentration of the sample relative to the buffer components, and independent of the tube diameter. One-dimensional numerical results for the separation of seven species in a sodium acetate buffer are presented to illustrate the effect. A detailed discussion of methods to control it is also presented. It is suggested that both wall adsorption of sample species and most coating methods used to control it or to reduce electroosmosis can be understood as aspects of the Debye double-layer theory. Large molecules, with a high degree of ionization with the opposite sign to the wall charge, are preferentially attracted to the layer, excluding smaller molecules, and decreasing the wall potential and mobility. We demonstrate the importance of choosing a combination of pH and tube material such that the wall and the large proteins in the sample have the same charge sign and repel each other.

The diffusion enhancement analysis is based on the analytic approximation of balancing the flow and mobility disturbance terms in the concentration equation for a sample species with the transverse diffusion term. This determines the fluctuating part of the concentration, with zero transverse average. The interaction of this concentration distribution with the fluctuations modifies the equation for the transverse average of the concentration, by adding a diffusivity $a^2 Y^2 / 48 D_i$. Here a is the radius, D_i is the diffusivity of the species, and Y is a disturbance speed and is a sum of contributions from the pressure-gradient-driven Poiseuille flow, the transverse mobility variation due to the heating in the tube, and other effects which we believe are smaller. The numerical factor of 48 is exact for the Poiseuille flow and the transverse mobility variations effects, and presumably it improves the estimate for the other effects.

The Poiseuille flow profile is driven by variations in the electroosmotic slip velocity, which are mostly caused by conductivity variations along the tube and by

changes in the Debye layer structure associated with composition changes along the tube. Contributions from temperature or radius variations along the tube are estimated, and are apparently smaller.

Relatively insignificant causes of dispersion include sample dispersion by the difference between the electroosmotic flow and the slower flow in the Debye layer (the layer is too thin), variations in the tube radius, and convection and electrohydrodynamics flows. Molecular diffusion is important (and theoretical plate numbers are achieved) if other dispersion effects are small; it is larger for sample species with small molecules.

INTRODUCTION

Capillary zone electrophoresis is a popular and convenient application of electrophoretic separation on a diagnostic scale, using a free fluid in a capillary tube. Flow, concentration and temperature disturbances are minimized by the small dimensions. The method's success derives from its convenience, reproducibility, resolution and speed, in comparison with available alternatives.

Electrophoretic separation (zone electrophoresis) is based on the differing mobilities of the components of a mixture, at a relatively low concentration, with sample applied locally in a buffer of fixed conductivity and pH. This contrasts with isoelectric focusing, in which there is no buffer, and mixture components focus to their isoelectric point, either in an immobilized pH gradient (ampholyte gel of varying composition) or in a mixture of ampholytes (which focuses to a pH gradient). Isoelectric focusing is relatively very slow. Both methods, especially isoelectric focusing, usually require some hydrodynamic control (either gel or capillary-type dimensions or stratification or rotation) to restrict undesirable flow effects.

On a diagnostic scale, zone electrophoretic separation can be performed as a batch process in a gel (gel electrophoresis) or in a free fluid in a thin tube (capillary electrophoresis). The sample is applied initially at a single point. On a larger scale, it can be done as a batch process in a rectangular chamber or gel, with the sample applied as a line normal to the field. For continuous flow electrophoresis, a buffer flows up a rectangular chamber, normal to the applied field. The sample is injected as a single thin column through a port at the bottom, separates on the way up the chamber, and is collected in outflow ports at the top.

The system of equations for electrophoresis described in the section Equations of electrophoresis applies to all processes. They are applied to capillary zone electrophoresis in the section One-dimensional application to capillary electrophoresis. The section Electrokinetic dispersion discusses electrokinetic dispersion and describes a numerical application.

Hydrodynamic effects

For many methods, separation can be degraded by hydrodynamic effects. Any irregular flow field disperses a single chemical species, and with multiple species their resulting distributions tend to overlap. The flow is driven by four main effects.

(i) Convection involves the effect of gravity on horizontal density variations. These density variations are due either to concentration differences or to temperature variations from ohmic heating and cooling at the walls.

(ii) Electrohydrodynamic flows are driven by the electric field in the fluid interior. They may be significant when there are variations along the field in either the dielectric constant or the conductivity. They have not been considered by earlier workers, but we have demonstrated in other work that they play a significant role in a continuous flow device¹.

(iii) Wall electroosmosis is associated with charge double-layers at the walls of an electrophoresis chamber. Ions either go into solution from the wall, or react chemically with the wall material, so that the wall is charged. Charge neutrality is maintained by a net charge imbalance in a Debye layer, with a thickness of order 100 \AA , next to the wall. The field component along the wall produces an enormous force on the charge in this layer, and gives rise to a shear layer. To an excellent approximation, the net effect is a slip velocity for the fluid at the wall (outside the layer), equal to the product of the tangential field with a wall mobility. Unless the ends of the chamber are open and the volume flux driven by this wall velocity is uniform, large pressure gradients will be produced, to drive an additional flow between the walls and satisfy continuity.

(iv) The fourth hydrodynamic effect applies only to a buffer flow or continuous-flow apparatus. The flow profile in the chamber is driven by a pressure gradient, and satisfies a no-slip condition on the chamber walls. Thus fluid near the walls has a longer residence time in the chamber than fluid near the mid-plane. The species therefore have time to move further in response to the transverse electric field, degrading separation.

Hydrodynamic effects alleviation

All four hydrodynamic effects can be effectively eliminated by the use of a porous medium (usually a gel). There is still a flow through the pores, closely related to electroosmosis, but it is not normally a major problem. This method excludes the continuous-flow technique; it has otherwise been highly successful. The unsatisfactory features of porous medium techniques are the time they currently require, the difficulty in making the gel medium in a reproducible manner, and sample-gel interactions, such as the difficulty in removing the separated materials from the medium for further testing.

Convection effects are effectively eliminated in the microgravity environment of space. They can otherwise be reduced by reducing the appropriate dimensionless Rayleigh number. This requires using some combination of small horizontal density differences, small dimensions, and a large viscosity.

Electrohydrodynamic flows are proportional to the gradients of the conductivity and dielectric constant, and to the squares of the field and of the linear dimensions. The variations are normally proportional to the sample concentration, relative to the buffer, and are therefore directly related to the throughput. Decreasing the field reduces the significance of these flows, since separation is proportional to the field strength.

With given convective and electrohydrodynamic forces balanced by viscous forces, the corresponding flows are proportional to the square of the spatial dimensions and inversely proportional to the viscosity. Decreasing the dimensions naturally decreases throughput; this is of course the basis for capillary electrophoresis, the subject of the present study. Additives with neutral charge have been used to increase the viscosity.

Wall electroosmosis can be decreased by the use of appropriate wall coatings, but the coatings are hard to apply uniformly and tend to deteriorate under the action of large fields. It is not a problem unless it leads to a Poiseuille flow profile through continuity and the resulting pressure gradients. So the chamber ends (in the field direction) must be open and the conductivity and wall properties must be uniform. Errors in the uniformity of the chamber width are not normally a problem, *cf. Temperature distribution*.

Electroosmosis-driven profile effects can also be minimized in a vertical column by the use of strong density stratification (normally with a sugar solution).² This confines the bulk of the vertical motion to a thin layer (much thicker than the Debye layer, but much thinner than the tube dimensions).

If an electroosmosis-driven Poiseuille profile is not avoided, its effect can be minimized by applying the sample as close as possible to the axis or center-plane of the chamber.

Sample dispersion due to residence-time variations in the Poiseuille flow profile up a continuous-flow chamber can be avoided only by applying the sample near the center-plane or by using chamber walls which move in the flow direction (instead of driving the flow by a pressure gradient)³.

Capillary electrophoresis

In conventional (open-tubular) capillary electrophoresis, a capillary tube (with a length of order a meter) containing buffer connects two electrode chambers filled with buffer. To introduce a short slug of sample to the tube, one chamber (normally the anode) is temporarily replaced by a chamber containing the same buffer with a low concentration of sample added. The electric field, and the associated electroosmotic plug flow, pull a short segment of buffer and sample into the tube. The original electrode chamber is then restored, and the electrophoresis continues. The separated components are normally detected near the other end of the tube by sensitive measurements of their fluorescent response to ultra-violet light. Other detection methods can be used. By replacing the electrode chamber, it is possible to collect or further analyze the separated components at the outflow end.

Development tests with this method have shown that successful operation requires capillary diameters of order 200 μm or less. This is consistent with the discussion in the previous subsection on methods for alleviating flow problems in electrophoretic separations.

In favorable conditions, up to 100 sample components can be distinguished.

EQUATIONS OF ELECTROPHORESIS

The system of equations described in this section are those in use in the computer model and code SAMPLE which we have developed and are currently upgrading from two to three spatial dimensions (plus time). This system and code have already been validated by application to experiments in a porous film with hemoglobin in a sodium barbiturate buffer, and by alternating-current electrohydrodynamic experiments in a continuous-flow configuration using a barbiturate buffer and a sample consisting of latex microspheres in a barbiturate buffer with a different conductivity.

An equivalent system (excluding the hydrodynamics) was used previously in

one-dimensional computer simulations by Bier *et al.*⁴. Other studies of aspects of electrophoresis modelling are listed in refs. 5–9.

For descriptive purposes we will use unrationalized electrostatic units based on the centimeter and gram. For reference, a volt is 1/300 e.s.u., while a coulomb is $3 \cdot 10^9$ e.s.u. Concentrations are expressed as usual in term of molarity, which is equivalent to mmol/ml. The description of the numerical results uses volts, according to convention.

Electrochemistry (pH determination)

In this model chemical reactions between the ions are totally neglected, with the exception of the equilibria between the ions of a particular species and the hydrogen and hydroxyl ions.

The pH distribution is determined from charge neutrality. The charge density is everywhere negligible compared with its components. Thus

$$[\text{H}^+] - [\text{OH}^-] + \sum j c_{ij} = 0$$

Here c_{ij} is the molar concentration of the chemical species i , ionized j times (where j is a positive or negative integer). Typical species are sodium, acetate, and hemoglobin. The total charge density (mmol/ml) is the sum of the contributions from the hydrogen ions, the hydroxyl ions, and all the other ions.

We can define the mean ionization and mean square ionization for each chemical species using the equations

$$c_i m_i = \sum j c_{ij}$$

$$c_i M_i = \sum j^2 c_{ij}$$

where the total species concentration is

$$c_i = \sum c_{ij}$$

These quantities m_i and M_i can be determined for each species as a function of H , using titration and other data and the concepts of chemical equilibrium.

The equilibrium between the hydrogen and hydroxyl ions is expressed by the familiar relation

$$\text{H}[\text{OH}^-] = C_{\text{OH}}$$

where we are now using H for the hydrogen ion molarity $[\text{H}^+]$. The pH is of course $-\log \text{H}$, using the base 10.

For sodium, chloride, and similar species, m_i and M_i are normally taken as constants.

The ionization equilibrium for a weak monovalent acid HA is expressed as



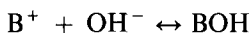
$$\text{H}[\text{A}^-] = K[\text{HA}]$$

where K is the ionization constant. Hence

$$M = -m = \frac{[A^-]}{[A^-] + [HA]} = \frac{K}{H + K}$$

Half the acid is ionized when $H = K$, or $\text{pH} = \text{p}K$.

The ionization equilibrium for a weak base BOH is



$$[\text{B}^+][\text{OH}^-] = C[\text{BOH}]$$

where C is a constant. Hence

$$M = m = \frac{[\text{B}^+]}{[\text{B}^+] + [\text{BOH}]} = \frac{H}{H + K}$$

where K is now C_{OH}/C . Half the base is ionized when $H = K$, or $\text{pH} = \text{p}K$.

Similar expressions are used for multivalent acids and bases, and for simple ampholytes such as histidine, where the ionization constants can be determined.

For complex proteins such as hemoglobin, with mean ionization between plus and minus 30 or more, depending on the pH , the ionization constants cannot be determined. Instead, we use for our model an analytic formula for m_i , with 13 constants. These constants are then chosen to give the best possible least-squares fit to measured titration data for m , at equally spaced pH values over a relevant range (say 41 values at intervals of 0.2 from 5.0 to 9.0). We are able to obtain formulas for m_i as a function of H with root mean square errors of about 0.1 compared with the measured data.

It can be shown that

$$M_i = m_i^2 + H dm_i/dH$$

For from an argument similar to those above for a weak acid or base,

$$C_{j+1} = C_j H / K_j$$

where C_j is the concentration of species C ionized positively j times, and j can be positive or negative. Hence

$$C_j = a_j H^j C_0$$

where the constants a_j involve the constants K_j . Thus

$$m = \frac{\sum j C_j}{\sum C_j} = \frac{\sum j a_j H^j}{\sum a_j H^j}$$

$$M = \frac{\sum j^2 C_j}{\sum C_j} = \frac{\sum j^2 a_j H^j}{\sum a_j H^j}$$

Hence, using logarithmic differentiation,

$$\frac{H}{m} \frac{dm}{dH} = \frac{\sum j^2 a_j H^j}{\sum j a_j H^j} - \frac{\sum j a_j H^j}{\sum a_j H^j} = M/m - m$$

which is the required result.

Finally, the H distribution is uniquely determined by the local total concentration values c_i , using the charge neutrality equation in the form

$$H - C_{OH}/H + \sum c_i m_i(H) = 0$$

Note that in this equation, every term increases with H (or decreases with pH), so the solution is unique.

Electrokinetics

The velocity through the water of an ion of species i with degree of ionization j is

$$jU_{ij}E$$

Here U_{ij} is the (positive) intrinsic mobility, or mobility per degree of ionization (cm/s/e.s.u.-field), and will be approximated as U_i (independent of j).

This velocity should be multiplied by an activity coefficient which is unity at low total ion concentrations and smaller for high concentrations; formulations have been given by Debye, Huckel, Onsager and Henry (as quoted in ref. 6). For simplicity, we will not discuss activity effects further in this study.

The vector flux of these ions, in mmol/cm²/s, is the sum of three terms, due respectively to the fluid motion, the ion motion through the fluid, and molecular diffusion of the ions,

$$F_{ij} = c_{ij}(\mathbf{u} + jU_i E) - D_i \nabla c_{ij}$$

Here the diffusivity D_i (cm/s) is taken like U_i as independent of j , and can be expressed using the Einstein formula as

$$D_i = U_i RT/F$$

where R is the gas constant (erg/degree/mmol), T is the absolute temperature, and F is the farad (e.s.u.-charge/mmol). This flux expression, with appropriate notation changes, applies to the hydrogen and hydroxyl ion fluxes as well.

From chemical species conservation (neglecting chemical reactions),

$$\partial_t c_i + \nabla \cdot \mathbf{F}_i = 0$$

where the total flux of species i is

$$\mathbf{F}_i = \sum \mathbf{F}_{ij} = c_i(\mathbf{u} + U_i m_i E) - D_i \nabla c_i$$

This equation determines the evolution in time and space of the chemical species concentrations.

Electric field

The total current density can be obtained by summing all the ion flux contributions, including those from hydrogen and hydroxyl, as

$$\mathbf{j} = \sigma \mathbf{E} - \nabla \Omega$$

where the conductivity and the ion diffusion current potential are

$$\sigma = F(HU_H + [\text{OH}^-]U_{\text{OH}} + \sum c_i U_i M_i)$$

$$\Omega = RT(HU_H - [\text{OH}^-]U_{\text{OH}} + \sum c_i U_i m_i)$$

The total contribution to the current density from the fluid velocity term is zero, using the charge neutrality condition derived earlier. If all the mobilities were equal, this condition would also make the ion diffusion current potential zero.

To close the system of equations for the electric field, we use the two conditions

$$\mathbf{E} = -\nabla V$$

$$\nabla \cdot \mathbf{j} = 0$$

From Maxwell's equations, \mathbf{E} is minus the gradient of the electric potential V (in e.s.u.). The net charge density is negligible compared with its components, so the divergence of the current is zero.

Debye layer

At any solid surface, an electrolyte forms a charge double-layer. Either some of the solid material goes into solution, or ions from the solution react chemically with the surface. The net effect is a charge density Q (e.s.u./cm²) on the surface, where Q depends in general on the solid material and the electrolyte material (particularly its pH). Q is negative for most practical materials (silica, glasses) at useful pH values.

The wall potential V_b is sometimes referred to as the zeta potential for the surface. We believe that Q is the more relevant surface property for an electrically insulated wall, and can often be regarded as a constant or as a function only of the pH. The quantity V_b varies much more with the concentrations in the fluid. In general, of course, neither Q nor V_b can be regarded as a property just of the wall material. Note also that the wall pH can be very different from the interior value.

This charge density Q is cancelled by a volume charge density in a very thin Debye layer against the solid boundary. We will find that the layer thickness is comparable with the dimensions of large proteins, so a continuum theory has limited validity. This is discussed further after we derive the continuum results.

We approximate this layer using a one-dimensional model, with $y > 0$ in the fluid (thus for a capillary of inner radius a , y is $a - r$). The y component of each ion flux is negligible compared with its components, and the advective flux is zero. Thus for the

concentration c of any ion, with degree of ionization j (this includes hydrogen and hydroxyl),

$$cjUE_y - Ddc/dy = 0$$

and substituting $E_y = -dV/dy$ and the Einstein diffusivity gives

$$c = c_\infty \exp [-j(V - V_\infty)F/RT]$$

Here V_∞ and c_∞ are the voltage and ion concentration outside the layer. The voltage outside the layer is not taken as zero, because of course it varies along the layer in electrophoresis.

Note that the hydrogen ion concentration is changed by the factor

$$H/H_\infty = f_H = \exp [-(V - V_\infty)F/RT]$$

and that all other concentrations are changed from their values outside the layer by the factor f_H . In particular, the hydroxyl ion concentration and the concentrations of any particular species at different j values continue to be in equilibrium with the local H value.

The total charge density (e.s.u./ml) in the layer is the sum

$$q = \sum j c_\infty F \exp [-j(V - V_\infty)F/RT]$$

interpreted to include the hydrogen and hydroxyl ion terms. Outside the layer, this sum is zero,

$$\sum j c_\infty F = 0$$

from the earlier condition of net charge neutrality.

From Maxwell's equations, the divergence of the displacement vector $D = \epsilon E$ is

$$- \epsilon d^2 V/dy^2 = 4 \pi q$$

where ϵ is the dielectric constant (about 80 for dilute aqueous solutions), and the electric permittivity of a vacuum is one in our units. Hence

$$d^2 V/dy^2 = - (4 \pi F/\epsilon) \sum j c_\infty \exp [-j(V - V_\infty)F/RT]$$

Multiplying by dV/dy , integrating, and using the boundary condition that dV/dy is zero outside the layer, gives

$$(dV/dy)^2 = (8\pi RT/\epsilon) \sum c_\infty \{ \exp[-j(V - V_\infty)F/RT] - 1 \}$$

The derivative of V at the boundary $y=0$ is determined by the condition

$$D_y = - \epsilon dV/dy = 4\pi Q$$

and has the opposite sign from Q . Taking the positive square root for consistency with negative Q (without real loss of generality),

$$\int \frac{dV}{\{\Sigma c_{\infty} \exp [-j(V - V_{\infty})F/RT] - c_{\infty}\}^{\frac{1}{2}}} - (8\pi RT/\epsilon)^{\frac{1}{2}} dy = 0$$

This integral can of course be evaluated numerically, for any particular set of concentrations. It is reasonably straightforward analytically in two special cases.

First, if the concentrations outside the layer are c for $\pm j$, and are otherwise zero, then the sum of exponentials simplifies, and

$$dV/dy = - (32 \pi c RT / \epsilon)^{\frac{1}{2}} \sinh[j(V - V_{\infty})F/2RT]$$

Here the sign choice is determined by the requirement that the solution V be finite at infinity. The excess potential V_b relative to infinity ("zeta potential") at the boundary is given by

$$\sinh(jV_b F/2RT) = (\pi/2 \epsilon c RT)^{\frac{1}{2}} Q$$

Integration and using this boundary condition yields the result

$$\log\{\tanh[j(V - V_{\infty})F/4RT] / \tanh(jV_b F/4RT)\} = -jF(8 \pi c/\epsilon RT)^{\frac{1}{2}} y$$

$$\tanh[j(V - V_{\infty})F/4RT] = \tanh(jV_b F/4RT) \exp(-y/\delta)$$

where the Debye layer thickness scale δ is given by

$$\delta^2 = RT\epsilon/(8\pi c j^2 F^2)$$

and is very small.

The second special case where integration is reasonably straightforward requires that the argument of the exponential function is small compared with unity, and is questionably valid close to the wall. The potential RT/F is about 25.6 mV. For realistic Q values and buffers, values of $(V - V_{\infty})$ comparable to or larger than RT/F are expected. The approximation is bad for larger values of $j(V - V_{\infty})$, and catastrophic if the larger values are negative. Consequences are discussed below. With this approximation, using

$$\exp x \approx 1 + x + x^2/2$$

and the condition of charge neutrality,

$$dV/dy = - (V - V_{\infty})/\delta$$

where the Debye layer thickness scale δ is now given by

$$\delta^2 = RT\epsilon/(4\pi IF^2)$$

and the ionic strength I is defined as

$$I = \sum c_{\alpha} j^2$$

(with the sum again interpreted to include the hydrogen and hydroxyl ion terms). For the first example, I is $2cj^2$. Thus the two δ definitions are consistent. Note that δ is very small (of order 10^{-6} cm), corresponding to a very thin layer. The solution is

$$V = V_{\infty} + V_0 [\exp(-y/\delta)]$$

where V_0 is an integration constant, determined by Q . If the approximation is valid right to the wall, the boundary condition gives the wall potential

$$V_b = V_0 = 4\pi\delta Q/\epsilon$$

In general, the integral must be evaluated numerically. Physically, if Q is negative, then the positive charge density in the layer must integrate to cancel it and keep the normal field component zero outside the layer. The potential disturbance is negative in the layer, and the ion concentrations increase in the layer for positive j and decrease for negative j . This establishes both the positive charge and the negative potential.

For low concentrations of protein ions with large positive j values (say 30), in a buffer of ions with small $|j|$ values, this concentration increase can be by a very large factor f_H , so that a substantial fraction of the protein ions are in the layer. This is often called adsorption. There is no chemical bond; the protein molecules are electrically held by the charge on the wall. If the layer charge is dominated by the protein, the layer thickness and the wall potential V_b are reduced. Adsorption is reversible; the addition of strong caustic soda or potash raises the pH so that the protein charge is negative, and the molecules (or their denatured remnants) are repelled from the wall.

It is normally important to choose the combination of wall material, buffer and protein so that adsorption is avoided. This requires use of a buffer with a relatively large pH (7–11), so that no protein ions have a large positive j value. This has been confirmed experimentally¹⁰.

Alternatively, it is possible to coat the walls uniformly with a protein or protein-like material with an even higher value of j . In favorable circumstances, this can reduce protein adsorption to acceptable levels. It also decreases the electroosmosis.

It should be noted that a large protein molecule has a size comparable with the Debye layer thickness, which casts some doubt on our use of a continuum theory. Thus hemoglobin (molecular weight 64 000) has a dimension of about $0.5 \cdot 10^{-6}$ cm. The theory is reasonable if it predicts small protein concentrations in the layer (with negative charges). But if in a particular case the theory predicts molar hemoglobin in the layer (64 000 g/l), it is unrealistic. This point must be born in mind in interpreting observations and comparing with the continuum theory.

The Debye layer is very thin, and therefore does not modify the bulk electric field solution or the species flux component normal to the wall. Its main importance is the electroosmosis effect.

Electroosmosis

The electric field component parallel to the wall exerts a large body force on the non-zero charge density of the fluid in the Debye layer. This force is balanced by the viscous stress. The force towards the wall is balanced by a pressure gradient. Taking the tangential field as being in the z direction, the viscous balance is

$$0 = \mu d^2 w / dy^2 + E_z q$$

where E_z is the z component of the field (constant in the layer), μ is the viscosity, and q is zero outside the very thin layer. The solution for w , using a no-slip boundary condition at the wall $y = 0$, and a negligible-viscous-stress boundary condition at infinity, is obtained by comparison with the equation and boundary conditions for V , and is

$$w(y) = (E_z \epsilon / 4\pi\mu)(V - V_\infty - V_b)$$

The value at infinity (*i.e.*, just outside the layer) is

$$w = U_w E_z$$

where the wall mobility U_w is

$$U_w = - V_b \epsilon / 4\pi\mu$$

It can incidentally also be obtained by integrating by parts as

$$U_w = \int_0^\infty y q(y) dy / \mu$$

and is of order $-Q\delta/\mu$. Note that the integral of q is $-Q$, and that δ is the thickness scale of the Debye layer.

Variations in the wall mobility will play an important role in the next section. They can be caused by temperature changes, affecting μ , or by changes in the species concentrations, affecting V_b .

For practical analysis, the Debye layer can be neglected in the equations of motion, except that the normal no-slip boundary condition at a solid boundary is replaced by the imposition of the slip velocity, parallel to the local field, with the correct wall mobility. Similarly, it can be totally neglected in the electrochemistry and electrokinetics, provided it never contains a significant fraction of any important species. For example with a capillary diameter of $5000 \cdot 10^{-6}$ cm, the factor f_H must approach 5000 for some species, to cause trouble. Note that this can easily happen, if care is not taken to restrict the j values by an appropriate buffer choice.

Electrohydrodynamics and convection

The equations of motion of an incompressible viscous conducting fluid in Cartesian coordinates are

$$u_{k,k} = 0$$

$$\rho \partial_t u_k = \sigma_{kl,l} + \rho g_k$$

where u_k and g_k are the k Cartesian components of the flow velocity and gravity, ρ is the density, the comma k and l suffices denote differentiation with respect to x_k and x_l , and the use of repeated suffices implies summation from 1 to 3. The stress tensor is

$$\sigma_{kl} = -\rho u_k u_l + \mu(u_{k,l} + u_{l,k}) + (\varepsilon/4\pi)E_k E_l - P\delta_{kl}$$

The first and second terms arise from momentum and viscosity. The third term is the electrohydrodynamic stress tensor, expressed using the Cartesian components of the field. The total pressure P is given by

$$P = p + (E^2/8\pi) [\varepsilon - \rho(\partial\varepsilon/\partial\rho)_T]$$

where $\varepsilon(\rho, T)$ is the dielectric constant, as a function of the density and temperature and p is the thermodynamic pressure. The electric terms are as given in ref. 11.

Assuming that the boundary conditions do not involve the pressure, it can be shown that the electrohydrodynamic term only modifies the flow if the conductivity or dielectric constant vary with position, and the gravity term only modifies the flow if the density varies with position. These variations are caused by temperature and concentration variations.

Temperature effects

The heat equation is

$$c_p D T / D t = K \nabla^2 T + \sigma E^2$$

where K is the thermal conductivity, D/Dt denotes the material derivative moving with the fluid, and c_p is the specific heat in erg/ml/degree Celsius. Viscous and chemical heating terms are negligible compared with the ohmic heating. This equation needs boundary conditions. The heat flux is of course continuous at interfaces. The same equation applies in the material of a solid container, except that there is no advection and ohmic heating is negligible. The thermal boundary condition at an air-cooled boundary is complicated (non-linear), unless insulation is a good approximation for the relatively short period of the experiment or forced-air cooling is used.

The resulting temperature distribution can modify the flow through convection, as described above. It also affects the separation, because many of the physical and chemical properties of the materials involved are functions of temperature. This includes the ionization properties involved in the electrochemistry and the pH determination, the mobilities of the species, the quantities determining the Debye layer and electroosmosis, and the viscosity. Normally, the viscosity variation (it decreases by about 2% per degree) is the most important; other parameters usually vary less than 0.5% per degree. The electroosmotic slip mobility and the individual species mobilities all vary inversely with the viscosity.

ONE-DIMENSIONAL APPLICATION TO CAPILLARY ELECTROPHORESIS

Our objective in this section is to use approximate analytic methods to quantify and compare the different effects which can contribute significantly to dispersion in capillary electrophoresis. We include in our analysis the effects of non-uniformities in the tube radius, variations in the wall mobility, and temperature variations along and across the tube. The coordinate z is measured along the capillary, and any bends are neglected. Transverse coordinates x and y can be chosen, or we use r for axisymmetric functions.

We introduce some notation at this point. For the temperature T , or any other variable, we define the transverse average T^A and the transverse disturbance T' by the equations

$$T^A(z) = \int T(x,y,z) dx dy / A$$

$$T'(x,y,z) = T(x,y,z) - T^A(z)$$

Here the integral is over the cross section area of the tube, at any particular z value, and

$$A(z) = \pi a^2$$

is the cross section area of the tube, with radius $a(z)$.

Electric current and field

Neglecting the ion diffusion current potential, we can write the z component of the current density along the tube, using Ohm's law, as

$$j_z = \sigma E_z = -\sigma \partial_z V$$

where E_z is the electric field component along the tube. In this equation, all variables are in general functions of position and time. Neglect variations of E_z across the tube. Then the total (area integrated) current along the tube is

$$J_z = A \sigma^A E_z$$

The equation of charge continuity implies that J_z is independent of z , though it can vary with time if the power supply is set to a constant voltage or power.

Temperature distribution

Temperature increases of $> 20^\circ\text{C}$ have been regarded as acceptable in capillary electrophoresis. Assume a steady-state solution where the heat generated along the tube escapes radially. The heat generation term is approximated as a function of z alone, in the form

$$\sigma E^2 = J_z^2 / \sigma^A A^2$$

Hence in the interior of the tube,

$$T = T_a + (J_z^2/\sigma\pi^2a^2)[(1-r^2/a^2)/4K + \ln(b/a)/2K_t + \ln(B/b)/2K_a]$$

where T_a is the ambient temperature, K , K_t , and K_a are the thermal conductivities of the water, tube and air, b is the outer radius of the tube, and B is a nominal radius reached effectively by forced or free cooling air at temperature T_a . This last factor, $\ln(B/b)$, is necessarily approximate, and is important because K_a is small; it is probably about 3 for an enclosed experiment (free convection), and about 0.3 with strong forced-air cooling. The other logarithm factor is about 2 for thin capillaries. Active cooling with water or some electrically insulating fluid has not been generally used.

The transverse average and disturbance parts of this temperature are

$$T^A = T_a + (J_z^2/\sigma^A\pi^2a^2)[1/8K + \ln(b/a)/2K_t + \ln(B/b)/2K_a]$$

$$\begin{aligned} T' &= (J_z^2/\sigma^AA^2)a^2(1-2r^2/a^2)/8K \\ &= \Delta T(1/2 - r^2/a^2) \end{aligned}$$

The temperature difference between the axis and the wall is

$$\Delta T = (J_z^2/\sigma^AA^2)a^2/4K$$

which plays a significant role. Note that this is twice the maximum amplitude of the transverse temperature fluctuation. Values of order one degree are likely; ten degrees is usually impossible because T^A would be excessive. The total temperature rise may presumably be up to about forty degrees, limited by problems with denaturing proteins (or boiling the water).

Note that ΔT is in general a function of z and t , with relative variations determined by the variations of σ^A and a . These relative variations are limited to a few percent, if the separation is at all successful. Since it is ΔT itself that contributes to dispersion, its variations with z and t are not significant.

Note further that T^A is also a function of z and t , with relative variations determined by the variations of σ^A , T_a , a , b , and B . The biggest problem in keeping T^A uniform along the tube is likely to be the parameter B , since cooling conditions will vary and K_a is small. This may be an important reason for keeping the temperature rise small, so that its variations with B are small.

The dependence of T^A on σ^A is interesting, because the conductivity is proportional to the mobilities, which vary inversely with the viscosity, which decreases about 2% per degree of temperature rise. Thus temperature changes are self-stabilizing; a local hot spot has an increased conductivity, which decreases the heating.

Assuming the capillary is not run to a steady thermal condition before applying the sample, an adequate estimate of the decay time in reaching this temperature is $c_p b^2/K$, which with an outer radius of 0.3 mm gives only about 1 s. Similarly, assuming the sample and buffer are at temperature T_a on input, there is an extremely short entry length of order $c_p a^2 EU_w/K$ for the temperature to rise to its equilibrium value. In addition, any variations in J_z or in σ^A are likely to be on larger time or length scales.

Thus our assumption of a steady-state solution with the heat conducted out radially is good.

This is one of the advantages of capillary electrophoresis, and allows large electric fields, with rapid separations and good resolution.

Flow profile

We can write the electroosmotic slip velocity at the wall as

$$\begin{aligned} W &= U_w E_z \\ &= U_w J_z / A \sigma^A \end{aligned}$$

The flow profile along the tube is

$$w(r, z, t) = W + 2X(1 - r^2/a^2)$$

and includes an additional term driven by the pressure gradient $\partial_z p$ along the tube. The mean flow due to the pressure gradient is

$$X(z, t) = -a^2 \partial_z p / (8\mu)$$

where $\mu(z, t)$ is the transverse average viscosity. The volume flux along the tube is obtained by integrating with respect to r , and is

$$F_z = A(W + X)$$

This is of course independent of z , since the fluid is incompressible. The mean flow speed, averaged across the tube, is

$$w^A = W + X$$

and the rest of w (with zero transverse average) is

$$w'(r, z, t) = X(1 - 2r^2/a^2)$$

For an open tube, with $W(z)$ known at fixed t , $p(z)$ and F_z can be computed from

$$\partial_z p = -8\mu X/a^2 = 8\mu(WA - F_z)/Aa^2$$

and the boundary condition that p is given at both ends (normally atmospheric pressure). Variations with z of the first term in the bracket (the electroosmotic flux WA) are compensated for by the establishment of a pressure gradient along the tube, driving a Poiseuille profile addition to the electroosmosis flow. Note that for a closed tube, the flux F_z is zero, which determines p except for an added constant.

Assuming that the variations in WA are either fixed in time or small and local, the volume flux F_z along the tube is constant, and

$$X = F_z/A - W$$

From the above expression for W , the electroosmotic flux along the tube is

$$AW = U_w J_z / \sigma^A$$

Note that variations in the capillary tube radius do not lead directly to variations in the electroosmotic flux. Nor do variations in the viscosity caused by variations in the temperature T^A along the tube, since both U_w and σ vary inversely with the viscosity.

The conductivity and wall mobility can vary independently, due to T^A effects on other parameters besides the viscosity (perhaps 0.5% per degree), or due to the presence of the sample components (electrokinetic effects). The electrokinetic change in the conductivity is complicated, as discussed in the next section. The electrokinetic change in the wall mobility is potentially larger, both because the relative contributions of proteins to the ionic strength are potentially larger than the relative contributions to the conductivity and pH (compare the subsection *Theoretical aspects of electrokinetic dispersion*), and because if the buffer pH is less than the pI for some of the proteins present, their concentrations are significantly amplified in the Debye layer, and they change its structure.

An appropriate estimate for X is therefore difficult. We suggest

$$X = O(W\Delta T_L/200)$$

where ΔT_L is the amplitude of fluctuations in $T^A(z, t)$, but the actual value may be larger due to electrokinetic effects. $X = O \dots$ means X is of order...

General theory of enhanced diffusion

The general equation for the evolution of the total concentration of a sample species was derived earlier in the form

$$\partial_t c_i + \nabla \cdot \mathbf{F}_i = 0$$

where the total flux of species i is

$$\mathbf{F}_i = \Sigma \mathbf{F}_{ij} = c_i(\mathbf{u} + U_i m_i \mathbf{E}) - D_i \nabla c_i$$

We will now drop the i suffix, as we will be confining attention to a single species.

We write U for the bracketed term in \mathbf{F} , note that its normal component is zero on the wall, and split it into its z and transverse components,

$$\begin{aligned} U &= \mathbf{u} + U_i m_i \mathbf{E} \\ &= U_z \hat{\mathbf{z}} + U_2 \end{aligned}$$

where $\hat{\mathbf{z}}$ is the unit vector in the z direction, and U_2 has zero z component. We split c and U_z into their transverse averages and fluctuating parts, so that

$$\begin{aligned} c &= c^A + c' \\ U_z &= U_z^A + U_z' \end{aligned}$$

We neglect fluctuations in D (it varies with temperature), since they are small, and since the degenerate perturbation theory becomes so much more complicated without significantly changing the result.

Then the exact equations are obtained by averaging, and using the fact that the normal component of U is zero on the boundary, in the forms

$$\partial_t c^A + \partial_z [c^A U_z^A + (c' U_z')^A - D \partial_z c^A] = 0$$

$$\partial_t c' + \partial_z [c^A U_z' + c' U_z^A + (c' U_z')' - D \partial_z c'] + \nabla_2 \cdot [(c^A + c') U_2 - D \nabla_2 c'] = 0$$

where ∇_2 denotes the transverse components of the gradient vector. Assuming that c' is much less than c^A , because of the dominant transverse diffusion term, the c' equation can be approximated very accurately as

$$\partial_z [c^A U_z'] + \nabla_2 \cdot [c^A U_2 - D \nabla_2 c'] = 0$$

This can be rewritten as

$$D \nabla_2^2 c' = c^A (\nabla \cdot U - \partial_z U_z^A) + U_z' \partial_z c^A$$

The contribution to the bracket from the flow part of U is zero. Thus the bracket is electrokinetic.

The solution is

$$c' = V' c^A + W' \partial_z c^A$$

where the scalar functions V' and W' are the unique solutions of the equations

$$\begin{aligned} D \nabla_2^2 V' &= \nabla \cdot U - \partial_z U_z^A \\ &= \nabla \cdot \mathbf{E} m U - \partial_z (E_z m U)^A \\ &= \nabla_2 \cdot \mathbf{E}_2 m U + \partial_z (E_z m U)' \end{aligned}$$

$$D \nabla_2^2 W' = U_z'$$

with zero normal derivative and transverse average.

Substituting in the average equation gives

$$\partial_t c^A + \partial_z [c^A (U_z^A + U_E) - (D + D_E) \partial_z c^A] = 0$$

where the speed enhancement is

$$U_E = (V' U_z')^A$$

and the diffusivity enhancement is

$$D_E = - (W' U_z')^A$$

the minus sign being introduced so that D_E has the sign of a diffusivity and is positive.

The speed enhancement by the fluctuations can have either sign. It is of small significance, compared with the regular transverse speed average U_z^A . The diffusivity enhancement D_E is always positive, and has magnitude

$$D_E = O(a^2 Y^2 / 48D)$$

where Y is the approximate maximum magnitude of the transverse speed fluctuation U'_z . The factor 48 is exact when U'_z has the radial dependence $(1 - 2r^2/a^2)$, as in the following subsection, and therefore presumably improves the estimate in all cases, provided that U'_z varies on the scale a , and Y is its approximate maximum magnitude (rather than just its order of magnitude).

Enhanced diffusion by the flow and mobility profiles

The Poiseuille flow profile

$$w' = X(1 - 2r^2/a^2)$$

and the transverse fluctuations in the mobility due to temperature, given approximately by

$$U' = \frac{dU}{dT} (\Delta T/2) (1 - 2r^2/a^2)$$

determine the transverse speed fluctuation as

$$U'_z = Y(1 - 2r^2/a^2)$$

where

$$Y = X + E_z m \frac{dU}{dT} (\Delta T/2) \approx X - E_z m U \frac{\Delta T}{2\mu} \frac{d\mu}{dT}$$

The approximation for Y assumes that the variation of the mobility with temperature is dominated by the variation of the viscosity, to which it is inversely proportional. Hence

$$W' = a^2 Y (6r^2/a^2 - 3r^4/a^4 - 2)/24D$$

determined by the conditions that W' have zero average across the tube and zero normal derivative on its boundary. This leads to the enhanced diffusivity

$$D_E = a^2 Y^2 / 48D$$

which can easily be much larger than D , especially for large protein molecules (with D values of order 10^{-7} cm²/s). For equality, aY is approximately $7D$.

Note that for a closed tube, Y is dominated by $X = -W = -EU_w$, and

$$D_E = a^2 E^2 U_w^2 / 48 D$$

This emphasizes the advantage of open tubes. Note also that Y is dominated by the same term for the Debye layer flow profile. However, the corresponding W' solution is of order $Wa\delta/D$, and the contribution to D_E is negligible because the layer is so thin.

Convection and electrohydrodynamic flow

The dominant convection flow distribution is derived by balancing the disturbance gravity term with viscosity and an addition to the uniform pressure gradient, and by applying the no slip condition and the condition of zero mean disturbance flow along the tube. The solution is

$$w' = a^2 g_z \frac{d\rho}{dT} (\Delta T/\mu) (1 - 4r^2/a^2 + 3r^4/a^4)/48$$

where g_z is the component of gravity along the tube. This assumes that the tube is not horizontal everywhere; for a horizontal tube convection flows are even slower. This flow speed is very small, and the corresponding dispersion is negligible.

Estimating the dominant electrohydrodynamic flow is more difficult. The field is determined by the conductivity distribution. The dielectric constant changes with temperature, but this change goes with the coefficient of thermal expansion of water, and is thus negligibly small. If the conductivity is a function of z only, or of r only, there is no flow. However, since the viscosity variation is 2% per degree, and since systems in current use allow substantial temperature changes, the variations of conductivity are likely to be dominated by temperature effects, unless electrokinetics becomes very important. Detailed estimates show that electrohydrodynamic dispersion is also negligible in capillary electrophoresis.

ELECTROKINETIC DISPERSION

Electrokinetic spreading is complex, and not readily amenable to analysis. It is caused by using excessive amounts of sample relative to the buffer concentrations. Knowledge of how to control it, other than by successive reductions in the sample concentration, is still somewhat limited. We first present some results from a numerical simulation. This is followed by a brief analysis.

One-dimensional simulation of capillary electrophoresis

The results of a computer simulation of capillary electrophoresis, using the one-dimensional option of our SAMPLE code, are presented in this section. The capillary tube radius a was taken as uniform, and sufficiently small so that the diffusivity enhancement could be neglected.

The buffer was sodium acetate, with sodium and acetate millimolarities of 1 and 2 (which is slightly lower than commonly used). We took both the intrinsic mobilities U as $500 \cdot 10^{-6} \text{ cm}^2/\text{s/V}$, and used a pK of 5.00 for acetate (the true values are different). This gave the buffer a pH of 5.00852 and a conductivity of $100.3798 \text{ } \mu\text{mho/cm}$. Apart

from the effect of the hydrogen ions, the pH would be 5 and the conductivity 96.5 $\mu\text{mho/cm}$. In these units F is 96.5 C/mmol.

The capillary was initially filled with buffer. At time zero the left buffer chamber was replaced by a sample chamber for 2 s, with a positive electric field of 50 V/cm. The buffer chamber was then restored, and the same field continued. We used a constant positive slip velocity at the wall of 0.113 mm/s. Thus this was also the mean tube flow.

The concentrations of the buffer components in the sample were unchanged. The sample also had small added concentrations of glycine, glutamic acid, histidine, lysine, and three chemical variants of human hemoglobin A, with micromolarities 1 for the hemoglobin variants, and 2 for the first four species. Note that these hemoglobin concentrations are relatively high, at about 0.064 g/l each, compared with 0.023 g/l for sodium. The ionization properties $m(\text{H})$ were based on formulas giving accurate fits to reported titration data, as described above. The respective intrinsic mobilities U_i in units of $10^{-6} \text{ cm}^2/\text{s/V}$ were 300, 300, 300, 200, 10, 10, and 10; these rounded numbers differ slightly from the true values. The nine actual mobilities $U_i m_i(\text{H})$ (including sodium and acetate) are plotted in Fig. 1, over the pH range 4–10.

Table I shows the indicated functions for each of the nine species, and for hydrogen. This table assumes a positive field E of 50 V/cm and a pH value of 5.00. The

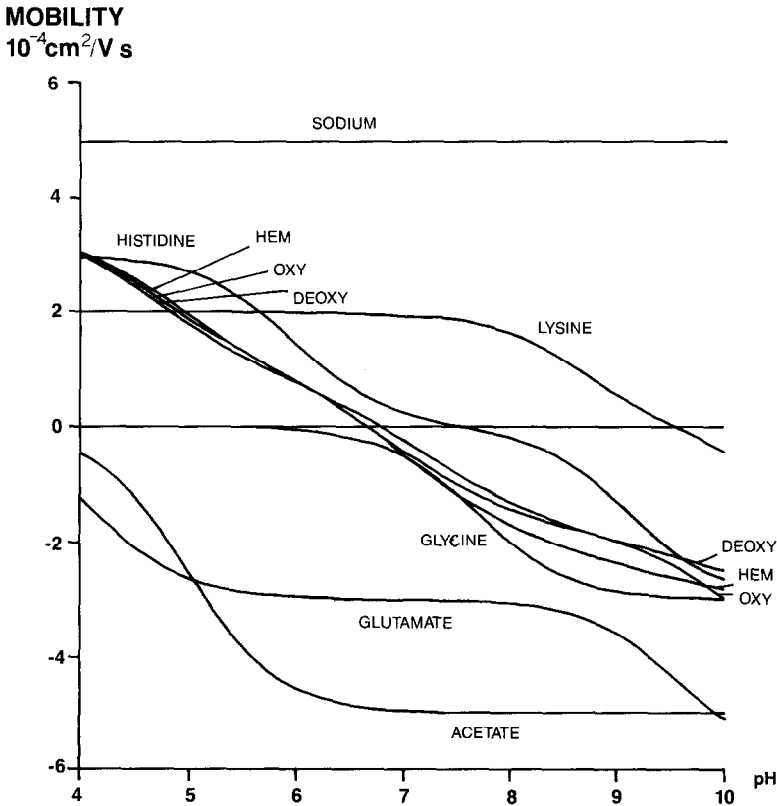


Fig. 1. Effective mobility plot for the nine species. HEM = Hemoglobin; OXY = oxyhemoglobin; DEOXY = deoxyhemoglobin.

TABLE 1
SPECIES PROPERTIES IN THE SAMPLE AT pH 5.00

Species	Intrinsic mobility, $U_i (10^{-6} \text{ cm}^2/\text{s/V})$	Mean ionization, m_i	Ion speed, $EU_i m_i (\text{mm/s})$	Concentration, $c_i (10^{-6} \text{ mmol/ml})$	Charge, $c_i m_i (10^{-6} \text{ mmol/ml})$	Ionic strength, $c_i M_i (10^{-6} \text{ mmol/ml})$	Conductivity, $c_i U_i M_i (10^{-12} \text{ mmol/cm/s/V})$
Sodium	500	1.0	0.2500	1000	1000.00	1000.00	50 000
Acetate	500	-0.50	-0.1250	2000	-1000.00	1000.00	50 000
Glycine	300	0.00	0.0000	2	0.00	0.01	0
Glutamic acid	300	-0.88	-0.1320	2	-1.76	1.77	53
Histidine	300	0.90	0.1350	2	1.80	1.81	54
Lysine	200	1.00	0.1000	2	2.00	2.00	40
Hemoglobin	10	19.49	0.0975	1	19.49	385.73	386
Oxyhemoglobin	10	18.99	0.0950	1	18.99	365.96	366
Deoxyhemoglobin	10	18.00	0.0900	1	18.00	329.42	329
Hydrogen	3600	1.00	1.8000	10	10.00	10.00	3600

ion speed through the fluid, in the third column, should be added to the fluid speed of 0.113 mm/s, to get the total motion through the capillary tube. The last three columns show the relative contributions to the charge neutrality condition, to the ionic strength, and to the conductivity. Note that the total charge micromolarity is about 70, requiring an increase in the pH (and thus particularly in the acetate ionization) for neutrality.

The following points should be noted in Table I.

(1) The assumed hemoglobin concentrations are rather large, for such a large molecular weight.

(2) The relative contributions of the hemoglobin types are very large for the ionic strength, due to the hemoglobin's large mean square ionization. This would modify the slip velocity and enhance diffusion in the field direction, as described earlier. In these tests, enhanced diffusion was not used.

(3) The buffer pH is between the pI of the wall and the pI of hemoglobin, which would be a bad choice, and would result in strong wall adsorption. The wall is negatively charged (since we assumed a positive wall slip velocity), while the hemoglobin is positively charged with a large mean ionization. A buffer with a pH of 7 or more would give better experimental results. This simulation did not even compute the Debye layer, so it was unaffected.

(4) The hemoglobin modifies the charge balance, and increases the proportion of the current which is carried by the acetate, as compared with the sodium, this results in significant changes in the sodium and (to a lesser extent) acetate distributions as the hemoglobin distributions move. Both species are depleted ahead of the hemoglobin and increased behind. As a result, the electric field is stronger ahead of the hemoglobin than behind it, and the front moves faster than the back. This is electrokinetic defocusing.

(5) The direct contributions of the hemoglobin types to the conductivity are small; the conductivity is changed much more by the change in the sodium concentration.

(6) Hydrogen ion contributions at this pH are relatively small; hydroxyl ion contributions are of course negligible.

(7) From the third column, glycine will move at the flow speed of 0.113 mm/s, while glutamic acid moves too fast in the negative direction to even enter the tube from the sample electrode chamber. The speeds of lysine and the three hemoglobin variants are very close (*cf.* Fig. 1), and they will take a long time to separate, but will eventually be in table order. The histidine will move out ahead of all the other sample species, with a combined speed of 0.248 mm/s.

(8) The total amount of each sample species which enters the tube from the sample electrode chamber is in proportion to the product of the time (2 s), the combined speed (column 3, plus 0.113 cm/s for the electroosmosis plug flow), and the concentration (column 4).

Computationally we used a non-uniform moving mesh, to resolve only the features of interest. We used 100-mesh intervals. We performed the computation up to a time of 6000 s, with the time step increasing from 0.01 s for the 2-s sample injection run, to 10 s for the last 5400 s. Computational error (such as computational diffusion) was minimal. Total concentration of each species was conserved, except when it crossed the computational boundaries. No negative concentration values occurred.

The use of sophisticated implicit methods ensured high accuracy and good computational efficiency. For our code, this was an easy problem; it is designed to operate in two or three spatial dimensions.

We have not yet programmed our code with the option to display functions of time at a fixed position along the tube. This is the form in which experimental capillary electrophoresis results are usually obtained, normally with a sensitive detector for ultraviolet absorption or for fluorescence. Our one-dimensional results are displayed as plots of particular variables as functions of z , at a fixed time. Usually, several of such plots are superposed.

Fig. 2 shows the sodium concentration, plotted at times in seconds of 1, 2, 4, 6, 8, 10, 12 and 14. The left boundary is the end of the tube, immersed in the sample electrode chamber for 2 s, and subsequently in the buffer chamber. Note that the sodium is depleted ahead of the hemoglobin, and increased behind. The nominal

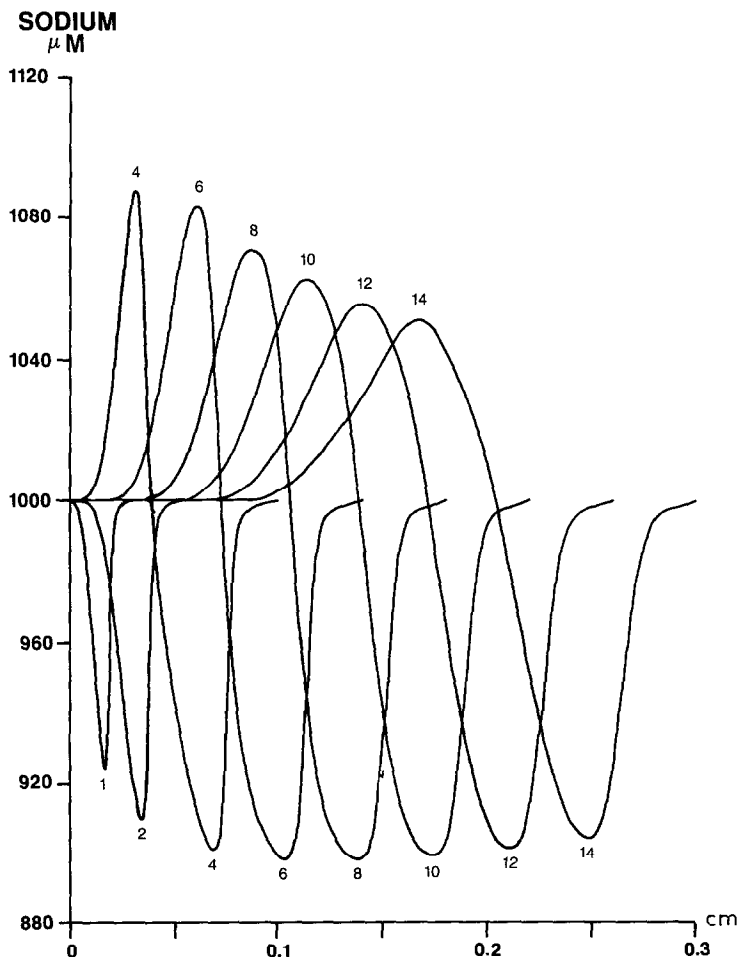


Fig. 2. Sodium distributions at early times.

buffer micromolarity is 1000, but after 4 s the maximum and minimum are 1088 and 900.5. Subsequently, the total range decreases slightly, but the width of the affected region continues to increase rapidly.

Fig. 3 shows the corresponding electric field distribution, plotted at the same times. The conductivity is proportional to the sodium concentration, to a fairly good approximation, and the electric field varies inversely with the conductivity. At 4 s the range is from 46 to 53 V/cm. With such large electric field variations, there are corresponding variations in the speeds of the ions through the water.

The three hemoglobin variants, and the lysine, are all close together at this stage because their speeds are so similar. They are in the region where the slope $\partial E/\partial z$ is positive, because the hemoglobin causes this region. Thus the front of their distributions move faster than the rear, and they are electrokinetically defocused. Apart from this phenomenon, the spreading of the hemoglobin variants would be very small in 14 s, because the diffusivities are so small.

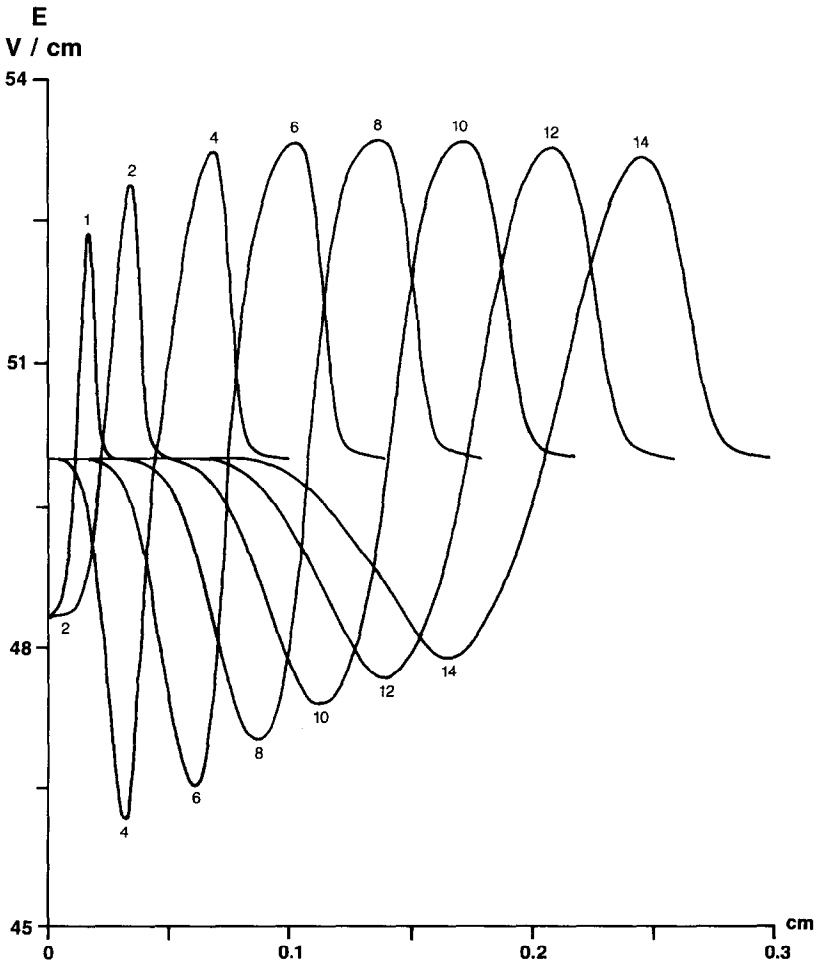


Fig. 3. Electric field distributions at early times.

In contrast, the histidine, which has a much smaller effect on the sodium and conductivity distribution and a higher speed, moves out ahead of the hemoglobin variants into the region of negative slope $\partial E/\partial z$, and the rear of its distribution moves faster than the front. Thus it is electrokinetically focused, and its peak concentration actually increases, instead of decreasing through diffusion.

To a first approximation, the sample species (excluding the glutamic acid) move to the right at the anticipated combined velocities of plug electroosmosis and electrokinetics (*cf.* Table I). They simultaneously spread through diffusion, particularly the smaller species which have much larger diffusivities. However, their concentration distributions are considerably modified by the focusing and defocusing effect described above. The electric field distortions result in considerable differences between the actual distributions of the sample species and the distributions which would result from the simple picture of superposing the effects of uniform electrokinetic speed, uniform plug electroosmosis, and simple diffusion.

The glycine is not ionized, *cf.* Fig. 1 and Table I. It moves along the tube with the plug electroosmosis flow, and diffuses in a straightforward manner, unaffected by the electric field. The glutamic acid has a negative combined speed (*cf.* Table I), and only a minute amount can enter the tube from the sample chamber through diffusion. It leaves rapidly once the sample chamber is removed and the boundary condition is changed, after the initial 2 s.

Fig. 4 shows the concentration distributions after 600 s, for lysine and the three hemoglobin variants. There is still considerable overlap, except between the two trailing variants. All four peaks have decreased from their sample values by a factor of approximately 4. The lysine has spread much less than expected, because as described earlier most of it is in the region ahead of the hemoglobin peak, where the slope $\partial E/\partial z$ is negative. The four distributions are all skewed to the right, due to the electric field maximum which stays near the middle of the hemoglobin. At a still later stage in the computation, these four species separate completely.

In conclusion, the simulation reveals some of the complex processes of electrokinetics, and part of the range of phenomena which can occur.

Theoretical aspects of electrokinetic dispersion

Electrokinetic spreading (or focusing) of a sample species in capillary electrophoresis is caused by variations in the mean ion speed Em_iU_i through the water, either due to variations in the mean ionization m_i of the species or due to variations in the electric field E .

The mean ionization varies only with the pH, depending on the slope dm_i/dH , (compare the slopes in Fig. 1). The electric field varies inversely with the conductivity. The pH variations arise from two causes: (a) the direct contribution of sample species; and (b) electrokinetic changes in the concentrations of the buffer species which maintain it. The conductivity variations arise from three causes: (a) the direct contribution of sample species; (b) changes in the ionization of buffer species induced by the change in the pH distribution; and (c) electrokinetic changes in the concentrations of buffer species which maintain it.

The electrokinetic changes in the concentrations of buffer species can clearly be regarded as also due to variations in the pH and conductivity.

For a two-component buffer consisting of a weak monovalent acid and strong

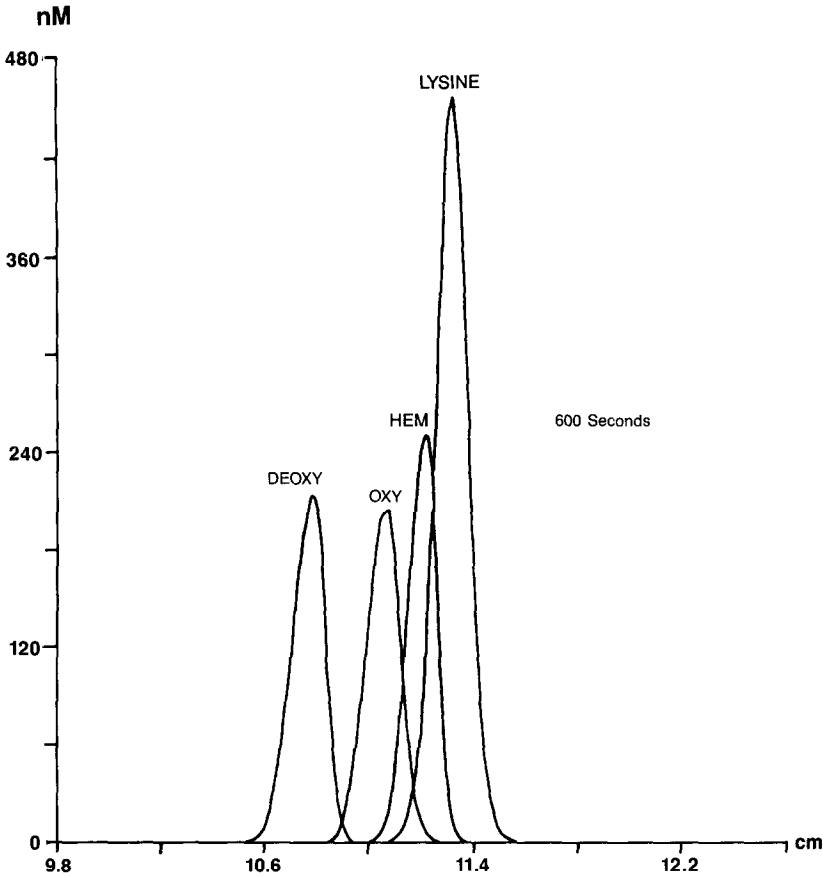


Fig. 4. Distributions of lysine and three hemoglobin variants at 10 min.

base (such as sodium acetate), it can be shown that provided hydrogen and hydroxyl are negligible in the charge balance and the conductivity, an arbitrary initial distribution of the two concentrations is not changed by the electrokinetics. The same applies to a weak monovalent base and a strong acid, and to a weak base and a weak acid. The proof uses the fact that $|m| = M$. It is a useful property, ensuring that buffer disturbances cannot grow without limit; but it is known that other buffer systems are stable too.

Most spreading occurs in the early stages, while the species are superposed and the concentrations are largest. In certain cases, the net effect is to focus the sample components more sharply. But this is generally followed by electrokinetic spreading at a later stage.

The electrokinetic effects of the sample species can be quantified as follows. In this discussion, note that

$$\text{pH} = -\log_{10}(\text{H}) = -\log_e(\text{H})/\log_e(10) \approx -\log_e(\text{H})/2.3$$

so that for any function m of pH or H,

$$dm/dpH = -H \log_e(10) dm/dH \approx -2.3H dm/dH$$

Also, the suffices s and b refer to the sample and the buffer, and the summations are over all the species in each. For the sample summation, the sum should be analyzed not only for the initial set of concentrations, but also for those which occur during the separation. The m and M values should be determined using the pH of the buffer.

The pH change due to the presence of the sample species can be approximated as

$$\Delta pH = - \frac{\sum c_s m_s}{\sum c_b dm_b/dpH}$$

Recall that the pH is determined by the condition of zero total charge density. The numerator is the sample contribution, while the product of the denominator with ΔpH is the change in the buffer contribution. The sum of these contributions is zero, which determines ΔpH .

The change in the conductivity due to the presence of the sample species can be approximated as the sum of two terms, the direct contribution of the sample species, and the change in the contribution of the buffer species, due to the pH change. The relative conductivity change is

$$\Delta\sigma/\sigma = \frac{\sum c_s U_s M_s + \Delta pH \sum c_b U_b dM_b/dpH}{\sum c_b U_b M_b}$$

The change in the pH leads to a corresponding change in the mean ionization of each species, and thus in its mean speed through the water. The relative change in the conductivity produces a relative change in the electric field strength, with equal magnitude and opposite sign. Both effects lead to focusing or defocusing of the sample species. Both effects also produce variations in the concentration distributions of the buffer species.

For comparison, the relative effect on the ionic strength (and thus on the Debye layer and wall mobility) is of order

$$\Delta I/I = \frac{\sum c_s M_s + \Delta pH \sum c_b dM_b/dpH}{\sum c_b M_b}$$

This relative change is normally larger than the two above, for large proteins, because the mean square ionization in the first term in the numerator can be so large, and there is no small intrinsic mobility as in the relative conductivity change.

The use of these parameters, in conjunction with the other dispersion effect criterion parameters, is discussed in the following section.

CONCLUSIONS AND RECOMMENDATIONS

Sample spreading in capillary electrophoresis is caused by direct electrokinetic effects, by wall adsorption, and by enhanced diffusion associated with electroosmosis

and pressure-driven flows and with variations in the intrinsic mobility due to temperature changes across the thickness of the tube. Variations in the diameter along the tube do not play a significant role. Variations in the temperature of a few degrees along the tube probably do not play a significant role. Electrohydrodynamic and convection flows are negligible.

Electrokinetic spreading of a sample species is caused by variations in the electric field and in the mean ionization of the species. The electric field varies inversely with the conductivity, and conductivity variations arise both from the direct contribution of sample species and from changes in the ionization of buffer species induced by the change in the pH distribution caused by the sample components. The mean ionization varies with the pH. The critical ratios presented in *Theoretical aspects of electrokinetic dispersion* determine the sensitivity of the buffer pH and conductivity to the sample species. Normally, if these parameters are kept small, electrokinetic dispersion should be limited.

Wall adsorption of the proteins is a problem when the wall and proteins have opposite charge, and the mean ionization of the protein is much larger than that of the buffer components. In extreme cases, practically all of the protein is adsorbed to the wall in the Debye layer. In less extreme cases, the preference of the protein for this layer results in "tailing", as the protein fails to keep up with the bulk of the electroosmotic flow.

Wall adsorption can be avoided by using a buffer with a pH not between the pI of the wall (typically 2 for silica or glasses) and the pI of the larger proteins in the sample. In practice, this means a pH of 7–10. Alternatively, the capillary or buffer can be deliberately loaded with a material which has an even larger positive degree of ionization at the chosen pH; this material is then preferentially adsorbed to the wall.

All other identified sample spreading mechanisms lead to an enhanced diffusivity for the species, with the form $a^2 Y^2 / 48 D_i$, where a is the capillary radius, Y is the disturbance speed amplitude, and D_i is the species diffusivity. The factor 48 is exact when the disturbance speed distribution is parabolic. The various mechanisms produce variations in the concentrations across the tube, which are kept small by diffusion. Spreading is decreased by decreasing the tube radius, or by decreasing the contributions to the disturbance speed Y . Note that for a typical large protein, D_i is of order $3 \cdot 10^{-7} \text{ cm}^2/\text{s}$, so the diffusivity is significantly enhanced if aY is of order $2 \cdot 10^{-6} \text{ cm}^2/\text{s}$ or more.

Electrohydrodynamic and convection flow speeds are negligible, for all conceivable capillary electrophoresis parameters. If they become significant, the separation is probably already a disaster because of other effects.

For flows driven by a pressure gradient along the capillary, Y is half the amplitude of the Poiseuille flow (which is the amplitude of the mean flow and of the disturbance). A forced Poiseuille flow, driven by an externally applied pressure difference, will only be satisfactory if a is very small. Variations of the wall slip velocity from its mean value along the tube lead to pressure gradients, and a Poiseuille flow profile in the tube, to keep the volume flux constant along the capillary.

Small variations in the tube radius do not lead to such a flow, because as the cross section area increases, the current density and field and electroosmotic slip velocity decrease, while the electroosmotic flux stays fixed. Similarly, variations in temperature along the tube result in an increased conductivity and an increased wall mobility, due

to the decreased viscosity; these effects cancel. There is a slight further increase in the slip velocity, due to the increase in RT and in the Debye layer thickness. The corresponding Y contribution is of order

$$EU_w \Delta T_L / T$$

where ΔT_L is the temperature difference along the tube from its mean value.

A temperature difference across the tube interior of ΔT will normally lead to a Y contribution of order

$$EmU \frac{\Delta T}{\mu} \frac{d\mu}{dT}$$

Note that the viscosity μ decreases about 2% for each degree of temperature. Here m and U are the mean ionization and the intrinsic mobility for the particular species, and we are assuming that the dominant temperature effect is the change in the viscosity, so the above expression can be rewritten as $EmU\mu\Delta T/50$.

We believe that other contributions are smaller, for practical parameter ranges. However, the formulas provided in this report allow them to be evaluated.

We now discuss the choice of the system and buffer for a given series of separations with similar sets of species present.

Provided the range of pI values for the species in the sample is not too high, the M_s and m_s values can be kept fairly small by an appropriate choice of the buffer pH. If there are large m_s values, they must all be positive (assuming the wall charge is negative), otherwise serious problems with wall adsorption, and consequent electro-osmosis variations and enhanced diffusion, can be expected.

To minimize electrokinetic effects, the parameters described earlier must be kept small. The simple method is to decrease the sample concentrations or to increase the buffer concentrations. The limit on decreasing the sample concentrations is normally detectability; there may be additional limits too. The buffer conductivity is limited, due to heating problems; again, there may be other limits on increasing the buffer concentration.

Ref. 10 reports the use of a buffer consisting of potassium chloride (to control the conductivity and make it independent of the pH) and an ampholyte (zwitterion) of low mobility (to control the pH without affecting the conductivity). The method seems attractive. As shown in *One-dimensional simulation of capillary electrophoresis*, there are problems with simple buffers where the same species provide both the buffering and the conductivity, such as sodium acetate. Note, however, that changes in the pH will affect the mean ionization of sample species even if they do not affect the conductivity. This will result in either focusing or defocusing.

Finally, it may be possible to decrease the enhanced diffusivity problems significantly by decreasing the temperature rise. A number of techniques are possible, besides the simplest of decreasing the electric field. Liquid cooling at the outside of the capillary is possible, but might make changing the capillary a difficult procedure.

SYMBOLS

ΔpH	change in buffer pH due to sample species
$\Delta\sigma, \Delta I$	changes in conductivity and ionic strength due to sample species
ΔT	temperature difference across the tube
ΔT_L	temperature difference along the tube
δ	Debye layer thickness scale
ϵ	dielectric constant
μ	fluid viscosity
ρ	density
σ	conductivity
σ_{kl}	Cartesian components of stress tensor, including momentum term
Ω	ion diffusion current potential
∂	partial derivative notation
∇	vector gradient operator
∇_2	transverse vector gradient operator, with no z component
'	following variable, denotes transverse fluctuation, with zero average across the tube interior
A	cross section area of the tube
\bar{A}	as superscript, denotes transverse average across tube interior
a	capillary inside radius
a_j	constants relating degrees of ionization
B	radius outside capillary where temperature is taken as ambient; near b for strong forced convection, but much more for weak free convection
b	capillary outside radius
b	as subscript, buffer
C_j	concentration of a particular species ionized positively j times
C_{OH}	product 10^{-14} of the hydrogen and hydroxyl ion molarities
c	concentration of a particular ion in the Debye layer
c_∞	concentration of a particular ion outside the Debye layer
c_p	specific heat
c_s	concentration of a sample species
c_b	concentration of a buffer species
c_i	total concentration of species i
c_{ij}	molar concentration of the chemical species i , ionized j times
D	diffusivity of a particular ion or species
D_E	diffusivity enhancement of a particular species
D_i	diffusivity of the chemical species i
D, D_y	electric displacement vector and component
E	electric field vector
E_k, E_l	Cartesian electric field components
E_y, E_z	electric field components
F_z	volume flux along the tube
F	farad (e.s.u.-charge/mmol)
F_i	vector flux of the chemical species i
F_{ij}	vector flux of the chemical species i , ionized j times
f_H	factor relating hydrogen ion concentrations inside and outside the Debye layer, a function of V

g_k, g_z	gravity vector components
H	hydrogen ion molarity [H^+]
H_∞	hydrogen ion molarity outside the Debye layer
I	ionic strength
i	as subscript, chemical species label
J_z	total current along capillary (independent of z)
j	as subscript, degree of ionization (integer)
\mathbf{j}	vector current density
j_z	current density along capillary
K	thermal conductivity of water
K_t, K_a	thermal conductivity of tube and air
K, K_j	ionization constants
k, l	Cartesian coordinate suffices (1–3)
M, M_i	mean square ionization of species i
m	mean ionization of species of interest
m_i	mean ionization of species i
$[OH^-]$	hydroxyl ion molarity
P	total pressure, including electrohydrodynamic terms
p	thermodynamic pressure
Q	surface charge density on solid wall (e.s.u./cm ²)
q	volume charge density (e.s.u./ml)
R	gas constant (erg/degree/mmol)
r	radius from the tube axis
s	as subscript, sample
T	absolute temperature in Kelvin
T_a	ambient temperature
t	time in seconds
U	intrinsic mobility of a particular ion
\mathbf{U}	vector speed for a particular ion
U_2	transverse vector speed for a particular ion, with no z component
U_E	speed enhancement
U_i	intrinsic mobility of the chemical species i
U_{ij}	intrinsic mobility of the chemical species i , ionized j times
U_H	mobility of hydrogen ion
U_{OH}	intrinsic mobility of hydroxyl ion (positive)
U_w	wall mobility associated with Debye layer and electroosmosis
U_z	z component of speed vector \mathbf{U} for a particular ion
\mathbf{u}	vector flow velocity
u_k	Cartesian component of the flow velocity
V	electric potential in e.s.u.
V'	scalar function for enhanced speed analysis
V_∞	electric potential outside the Debye layer
V_b	excess electric potential at the wall; zeta potential
V_0	integration constant for Debye layer; wall potential in linear case
W	electroosmotic slip velocity at the wall
W'	scalar function for enhanced diffusion analysis
w	fluid velocity component

w'	difference between flow along tube and its average
X	mean flow, and disturbance flow amplitude, along capillary due to the pressure gradient
y	distance from the wall; coordinate for Debye layer
Y	magnitude of speed fluctuation U'_z
z	coordinate measured along the tube
z	as subscript, refers to z component (along tube)
\hat{z}	unit vector in z direction

ACKNOWLEDGEMENTS

This work was partially supported by NASA contract NAS8-37342. We thank David N. Donovan for his contributions.

REFERENCES

- 1 P. H. Rhodes, R. S. Snyder and G. O. Roberts, *J. Colloid Interface Sci.*, 129 (1989) 78–90.
- 2 G. O. Roberts, in preparation.
- 3 P. H. Rhodes and R. S. Snyder, *U.S. Pat.*, 4 752 372 (June, 1988).
- 4 M. Bier, O. A. Palusinsky, R. A. Mosher and D. A. Saville, *Science (Washington, D.C.)*, 219 (1983) 1281–1287.
- 5 O. S. Mazhorova, I. P. Popov, V. I. Pokhilko and A. I. Feonychev, *Izvestiia, Mekhanika Zhidkosti i Gaza*, May–June (1988) 14–20 (in Russian).
- 6 R. A. Mosher, D. Dewey, W. Thorman, D. A. Saville and M. Bier, *Anal. Chem.*, 61 (1989) 362–366.
- 7 D. A. Saville and O. A. Palusinsky, *AIChE J.*, 32 (1986) 207–214.
- 8 O. A. Palusinsky, A. Graham, R. A. Mosher, M. Bier and D. A. Saville, *AIChE J.*, 32 (1986) 215–223.
- 9 R. A. Mosher, M. Bier and P. G. Righetti, *Electrophoresis*, 7 (1986) 59–62.
- 10 H. H. Lauer and D. McManigill, *Anal. Chem.*, 58 (1986) 166–170.
- 11 L. D. Landau and E. M. Lifshitz, *Electrodynamics of Continuous Media*, Pergamon Press, New York, 1960, p. 67.